Global electron content and solar activity: comparison with IRI modeling results

E.L. Afraimovich, E.I. Astafyeva, A.V. Oinats, Yu.V. Yasukevich, I.V. Zhivetiev

Institute of Solar-Terrestrial Physics SD RAS, Irkutsk, Russian Federation,
afra@iszf.irk.ru; http://rp.iszf.irk.ru/homepage/afra/

Abstract

We present the first results for investigation of the dynamics of global electron content (GEC) that is equal to the total number of electrons in the near-Earth space environment bounded by the GPS orbital altitude (about 20000 km). We propose a method of GEC estimation based on the Global Ionospheric Maps technique (GIM). GEC is calculated by summation of total electron content values multiplied by the area of a GIM cell, over all GIM cells. We have suggested the measurement unit GECU, which is equal to 10^{32} electrons. We analyzed data for the period 1998-2005 and we found that 27-day variations of GEC are very similar to the ones of the index F10.7, but GEC value lags about 30-60 hours as compared to the F10.7. It was also found out that GEC has seasonal variations; their maximum is related to equinoctial months.

We developed a method and software for GEC calculation using IRI-2001 (GEC-IRI) and we compared these results with experimental GEC values during the period from 1998 to 2005. We found a good agreement between experimental and model data for GEC in general, but there are also some significant distinctions. In particular, GEC-IRI values exceed experimental GEC values for upper integration height higher than 2000 km (up to 5-6 times for GPS satellites altitude, ~20000 km). Relative difference between GEC-IRI and experimental GEC series increase as smoothing time window decreases. Mainly this reflects the fact that IRI is a median ionosphere model and do not take into account day-to-day variations of the ionosphere parameters (e.g. 27-day variations).

Key words: GPS, total electron content, IRI, global electron content, solar activity.

1. Introduction

Earth's ionosphere is an important part of the near space environment; its condition is determined by the solar radiation fluxes within the different wavelength ranges (Ivanov-Kholodny and Nikolsky, 1969; Akasofu and Chapmen, 1972; Krinberg and Taschilin, 1984). After the first paper (Beynon and Brown, 1959), the attempts were undertaken to reconstruct the solar radiation characteristics from the ionosphere observational data (Nusinov, 2004). A necessity of the problem is still on, in spite of development of modern extra-atmospheric (satellite) facilities for solar radiation detection.

These researches are of a special significance nowadays due to development of solar-terrestrial physics. A number of questions of solar activity dynamics as a primary factor of the Earth climate change are to be solved.

Nowadays ionosphere monitoring is realized by different ground-based and satellite radio sounding instruments (Bryunelli and Namgaladze, 1988). It allows determining of local ionosphere

parameters, but they have significant global distinctions. This makes difficulties for estimation quantitative solar radiation characteristics from ionospheric data.

On the other hand, an adequate application of experimental data for modern solar radiation monitoring facilities is necessary for different ionosphere models correction (Klobuchar, 1986; Afraimovich et al., 2000; Giovanni and Radicella, 1990; Bilitza, 1990, 2001, 2004; Gallagher et al., 1988; Daniell et al., 1995; Huang et al., 2002; Radicella and Leitinger, 2001; Coisson and Radicella, 2004, 2005; Coisson et al., 2002, 2005). These models are widely used for ionosphere studying as well as for providing of effective satellite and ground-based radio system operating.

Afraimovich et al. (2006) for the first time proposed a new approach for solving these problems. It lies in determining of a global electron content that is equal to the total number of electrons in the near-Earth space environment (within the orbital altitude of the GPS-GLONASS navigation systems, about 20000 km). The method of GEC estimation and the certain software were developed at the Institute of Solar-Terrestrial Physics SD RAS. An advantage of this approach is in disappearance of local features of ionosphere parameters and in determining of the dynamics of global characteristics.

GEC as a generalized ionospheric parameter can be used not only for studying of the ionosphere and atmosphere processes due to solar activity changes, but also for solving the inverse problems, for example, estimation of the numerical characteristics of the ultraviolet solar radiation flux within the range 100-1000 Å (10-100 nm) and so on.

The objectives of this paper are to study the dynamics of global electron content during the 23rd cycle of solar activity and to compare the experimental results with IRI modeling data.

Sections 2 and 3 provide general information about the experiment and describe the methods of GEC calculation from IONEX data and using IRI-2001 model (GEC-IRI).

Sections 4–7 present our new evidence characterizing the dynamics of global electron content during the 23rd cycle of solar activity and consecutive comparison with IRI-2001 modeling results.

2. General information about the experiment. Method of Global Electron Content estimation

Our method is based on use of global ionosphere maps of total electron content (TEC) generated on a basis of data from International GPS receivers network (Mannucci et al., 1998; Schaer et al., 1998). Global TEC maps are calculated at several scientific centers: Geodetic Survey Division of Natural Resources Canada (EMRG) [http://www.nrcan-rncan.gc.ca/], Center for Orbit Determination in Europe, University of Berne, Switzerland (CODG) [http://www.cx.unibe.ch/], Jet Propulsion Laboratory of California Institute of Technology (JPLG) [http://www.jpl.nasa.gov/], Grup Universitat Politecnica de Catalunya (UPCG) [http://www.upc.es/], European Space Agency Group (ESAG) and others.

In spite of different methods for the absolute vertical TEC reconstruction used by different laboratories, the general idea is based on fitting of the optimal parameters of selected model of the vertical electron density distribution (N(h)-profile). For such model values of the expected ionosphere correction to the distance to a satellite are calculated for real visual angles to satellite. Then calculated correction values are compared with measured one and this process is repeated for

different ionosphere model N(h)-profile parameters as long as minimal discrepancy will be achieved that corresponds to RMS values presented in IONEX file. Then, for "optimal" N(h)-profile "vertical" TEC is calculated that is equal to average value of "vertical" TEC $I_{i,j}(t)$ for corresponding GIM (i,j) cell.

GIM are available in Internet at site ftp://cddisa.gsfc.nasa.gov/pub/gps/products/ionex/ in standard IONEX format; the files contain data of the vertical TEC from 0º to 360º of longitude and from -90º to 90º of latitude. A size of the elementary GIM cell is 5º of longitude and 2.5º of latitude. For each time moment the vertical TEC values $I_{i,j}$ can be obtained from two-hour time resolution IONEX files, where i and j indexes are the numbers of a certain GIM cell.

Global electron content G(t) is calculated by summation of the TEC values multiplied by cell's area $S_{i,j}$ over all GIM cells (Afraimovich et al., 2006)

$$G=\Sigma I_{i,j} \bullet S_{i,j} . \qquad (1)$$

Afraimovich et al. (2006) have suggested a unit of GEC GECU, which is equal to 10^{32} electrons.

GEC estimation accuracy is higher than TEC determination accuracy for each GIM cell (about 10-20% - Mannucci et al., 1998; Schaer et al., 1998), since averaging of independent TEC values is performed for the entire globe with the total number of GIM cells 5184. This allows us to reveal GEC variations and trends of only insignificant amplitude that is impossible in the case of TEC analysis in the separated GIM cell.

Our experiment is based on global IONEX database for a period 1998-2005 presented at (ftp://cddisa.gsfc.nasa.gov/pub/gps/products/ionex/). Comparative study showed that the results of GEC estimation do not depend on a concrete laboratory data.

Figure 1c presents GEC variations G(t) calculated using IONEX data of JPLG, CODG, ESAG, UPCG laboratories for the 1999. As one can see, G(t) series for different laboratories differ from one another only by constant value. The biggest difference (up to 0.2 GECU) was found for JPLG data. If we multiply the series G(t) by corresponding proportional coefficient, the average deviation between the series for 1999 will not exceed 0.05 GECU (panel d). However for 2001 and 2003 normalized series G(t) differ more sufficiently (panels a and b, respectively).

Relative GEC deviations (%) and RMS (%) in 1999-2005 for different laboratories data smoothed by 10-day window are also presented in the Table 1. The Table shows that relative GEC deviation changes from about 3% to 16%, depending on solar activity level. Maximal GEC deviations are found in the periods of minimal solar activity. At the same time RMS values change from about 2% to 6% and maximal RMS values are found for maximum solar activity period.

Thus we can conclude that global summation allows us to find systematic overestimation of JPLG TEC data relative to data of the other laboratories.

Hereinafter all calculations are carried out for JPLG data. In the case of JPLG data lack we used CODG data with the corresponding correction. Total number of calculated GEC values for 2771 days with two-hours time resolution is about $2771 \cdot 12 = 33252$.

Solar activity level can be estimated by several parameters characterizing solar irradiance and space weather near the Earth (http://www.drao-ofr.hia-iha.nrc-nrc.gc.ca/icarus/www/current.txt; http://www.spacewx.com). Here we selected F10.7 solar activity index F(t), which is equal to solar radiation flux on the wavelength 10.7 cm in s.f.u. units (10^{-22} Wm^{-2} Hz^{-1}).

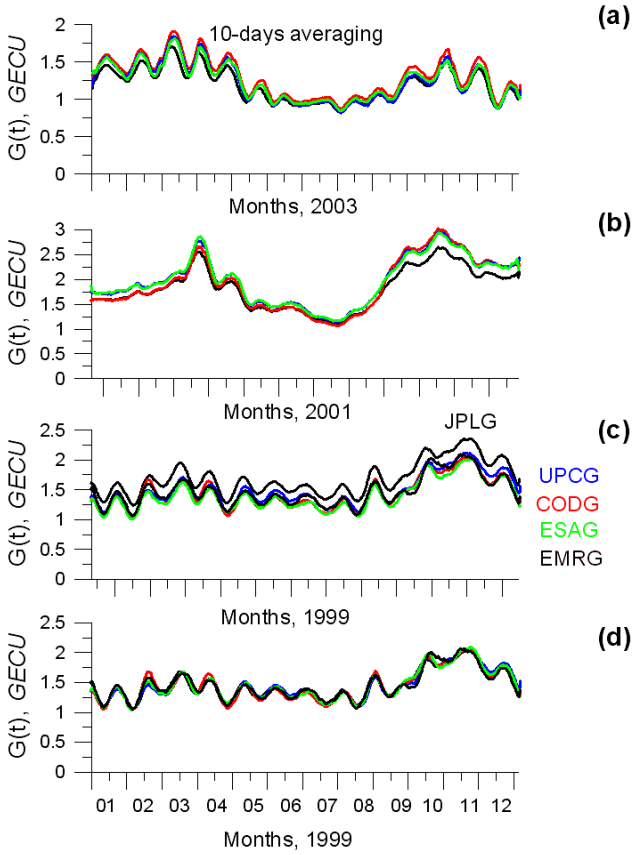

Figure 1: *(c) - GEC, calculated from the [JPLG, CODG, ESAG, UPCG] IONEX data for the 1999; (a, b, d) - the same that on (c), but for normalized GEC data for the 2003, 2001, 1999.*

Table 1: *Relative GEC deviations (%) and RMS (%) in 1999-2005 for different laboratories data smoothed by 10-day window*

N	Year	JPLG-CODG, %	JPLG-UPCG, %	JPLG-ESAG, %
1	1999	14,8 ± 2,3	12,1 ± 3,4	16,9 ± 1,7
2	2000	13,7 ± 2,9	3,2 ± 3,3	12,6 ± 3,6
3	2001	10,5 ± 5,2	4,2 ± 2,7	9,8 ± 2,8
4	2002	5,3 ± 5,8	4,6 ± 5,8	10,8 ± 4,5
5	2003	7,0 ± 2,5	9,4 ± 5,9	13,4 ± 2,7
6	2004	10,7 ± 7,3	10,9 ± 3,8	16,1 ± 3,6
7	2004	13,1 ± 1,9	12,6 ± 2,3	15,8 ± 3,0

Some important points in our work:

1. We use the term “global electron content” because GIM maps are presented for the entire globe. Actually TEC estimations near the geographical poles are very rough. For these regions the NOR maps presented at the site http://www.kn.nz.dlr.de/daily/tec-np/ are more representative. However, contribution of high latitude regions to GEC is essentially smaller than the one of middle and low latitudes. Thus, as the first approximation, G(t)

value calculated by formula (1) is sufficiently close to the total number of electrons around the Earth.

2. Here we study GEC dynamics due to solar activity changes within a part of the 23rd cycle (1998-2005) as well as related to the Sun rotation (27-days variations). Therefore, we smooth G(t) series with the time window of 10 days. Thus, G(t) is two-hours value of the 10-day running average of the GEC centered at each time moment. At the same time, diurnal variations appear to be averaged and, therefore, important effects of quick GEC changes cannot be distinguished (such as geomagnetic disturbances). But these processes are the topics of a special study.

3. Global Electron Content modeling

Obviously, for global electron content modeling we should use ionosphere model satisfying at least two conditions: (1) it must reproduce an electron density profile not only up to the maximum of F2 layer, but higher than the one; (2) it must be a global (i.e. it must reproduce TEC values or electron density profile at any point of the Earth globe). Lately there are known several certain ionosphere models. In particular, we can note such models as IRI (Bilitza, 1990; Bilitza, 2001) and NeQuick (Giovanni, 1990; Radicella, 2001; Leitinger et al., 2005). Both these models are recommended by International Telecommunication Union, Radiocommunication sector ITU-R (ITU2004) as suitable methods for TEC estimations.

Another critical moment for GEC modeling is also topside profile behavior of the ionosphere model. IRI-2001 electron density profiles are valid up to altitudes about 2000 km, NeQuick model is valid up to 20000 km. Recently intensive accuracy researches of the mentioned models have carried out based on the topside sounder satellite data (Huang et al., 2002). Many researchers have noted about essential overestimation of the electron density in the topside ionosphere by IRI-2001, especially for high latitudes (Coisson and Radicella, 2005; Bhuyan and Borah, 2005; Coisson and Radicella, 2004; Coisson et al., 2002). In a new version of IRI which expected to appear in 2006 the correction term of the topside density profile for the current IRI model will be included as proposed by D. Bilitza (2004). Furthermore NeQuick electron density topside will be included in the new IRI as an option for topside electron density calculations (Coisson et al, 2005).

For GEC modeling we chose well-known and widely used international empirical model of ionosphere IRI-2001 (http://nssdc.gsfc.nasa.gov/space/model/ionos/iri.html). For a certain location, date and time the model reproduces electron density, electron and ion temperature, and ion composition within the altitude range from 50 to 2000 km, as well as vertical TEC. IRI, which is a median model, takes into account diurnal and seasonal variations of the ionosphere parameters and is considered to be a standard for different ionosphere calculations. IRI model has many operational modes that differ in a set of input parameters. This permits to adjust the model for the specific purposes. IRI model can be used both on-line and by retrieving the FORTRAN source code via anonymous ftp server NSSDC (ftp://nssdcftp.gsfc.nasa.gov/models).

The main parameter in the case of TEC calculation in IRI-2001 is upper height for electron density profile integration h_{max}. Besides, it has an opportunity of choosing one of three integration modes that influence on the program run time and the accuracy of TEC estimation. In the default mode TEC integration is carried out with different step sizes from 1 to 30 km depending on the current integration height. To reduce the program run time we chose fast TEC integration mode with minimal accuracy (>5%), in which the exponential approximation of the electron density profile is

used within the height range from (hmF2+150 km) to h_{max}, where hmF2 is the height of F2 layer maximum. The storm model was turned off during calculations and the other input parameters were chosen like in the standard IRI mode.

For test GEC modeling we developed the certain software, GEC values (GEC-IRI) were calculated in two stages. At the first stage, IRI TEC values were calculated throughout the globe (or in the certain region) in latitude-longitude mesh points with step 5º along the longitude and 2.5º along the latitude during all time period with step of 2 hours. At the second stage, derived TEC values were integrated using the technique described earlier for GIM (Section 2, formulae (1)). Thus, we obtain time dependence of modeled GEC-IRI values M(t).

Calculations for the upper height h_{max} of GPS satellite orbit altitude 20000 km, as expected, showed a significant overestimation of GEC values (more than 6 times). Figure 2a presents model GEC values M(t) for 2003 year calculated for h_{max} = 2000, 10000 and 20000 km. The series were smoothed with 10-day time window.

Figure 2b also shows M(t) values for the year 2003, calculated for h_{max} 1000 and 2000 km (blue curves) and smoothed experimental GEC values G(t) (red curves). As we can see, the experimental GEC curve G(t) lies between the two modeled curves. Therefore, hereinafter all estimations will be performed for h_{max} =2000 km. As one can see, the shape of the model GEC curve is very similar to the experimental one with semi-annual GEC variations, but the modeled GEC values increase proportionally to h_{max}. As it was mentioned above, this overestimation is related to the fact that IRI electron density profile is close to the real ionosphere profile only up to the height of about 1500 km, but IRI electron density becomes almost constant above the height more than 1500 km.

4. Global Electron Content during the 23rd cycle of solar activity

GEC value G(t) shown in Figure 3a (orange curve) illustrates a considerable GEC variability during the 23rd cycle of solar activity: from 0.5 to 3.5 GECU.

Absolute GEC values themselves are of interest as far as they are obtained within the simple and physically founded model of refractive index of the ionosphere plasma (Hofmann-Wellenhof et al., 1992). This model links GPS signal phase and group delay with value of the total electron content along line-of-sight (LOS) between GPS receiver and satellite. From this point of view experimental GEC values are as important as maximum electron density values of E or F2 layers, which are determined from measurements of critical frequency at the ionosphere stations. Thus, it is possible to use GEC values as well as maximum electron density values for calibration of parameters of solar ultraviolet radiation models as well as of different ionosphere models.

A comparison with variations F(t) of solar activity F10.7 index that is equal to the 10.7-cm solar radio flux (Figure 3b) shows good agreement between these values. It is especially obvious from comparison between G(t), M(t) and F(t) dependencies smoothed by one-year time window (Figure 3d, red, blue and green curves, respectively).

Regression dependence of the global electron content from F10.7 index during the period 1998-2005 based on the data from figures 3a and 3b, is shown in Figure 4b. Smoothed GEC and F10.7 series regression (Figure 3d) is shown in Figure 4c. It is well approximated by linear dependence

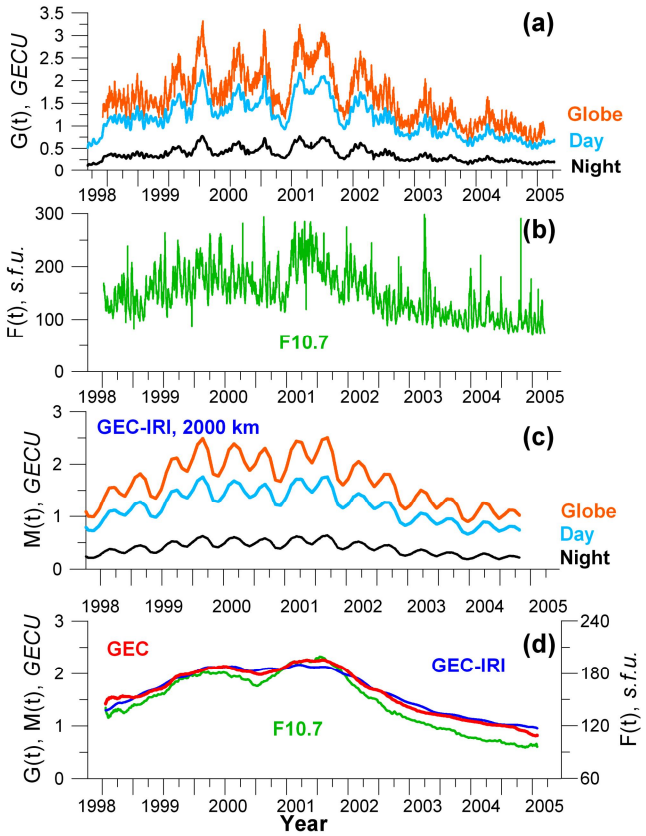

Figure 3: *(a) - GEC variations G(t); (b) - the 10.7-cm solar radio emission F(t); (c) - the IRI-2001 model estimation of GEC M(t); (d) - smoothed with the 365-day time window G(t), F(t) and M(t).*

$$G=0.013 \bullet [F10.7-60] + 0.5. \qquad (2)$$

This correlation is in quite agreement with similar formulas for the F2 ionosphere layer critical frequencies assumed in the modern empirical model of the ionosphere (Bryunelli and Namgaladze, 1988).

We calculated GEC-IRI using the IRI-2001 for h_{max} = 2000 km and compared them with experimental GEC values at the period from 1998 to 2005. GEC-IRI dependence M(t) for h_{max} = 2000 km is shown in Figure 3c (orange curve). Comparison between experimental G(t) and model M(t) series smoothed by one-year time window shows a good agreement between these values (Figure 3d, red and blue curves, respectively). The mean relative deviation [G(t)-M (t)]/G(t), %, between experimental G(t) and IRI model series M(t) for this time period does not exceed 1.5% with RMS about 5% (see Table 2, line 1).

Regression of smoothed GEC and GEC-IRI series during the period 1998-2005 (Figure 3d) is shown in Figure 4a. It is well approximated by linear dependence

$$G = 1.056 \bullet M + 0.1. \qquad (3)$$

Such a good agreement between experimental and model dependencies was obtained for the period 1998-2005 only for G(t) and M (t) series smoothed by the one-year time window. The difference becomes more significant when the smoothing time window is less (see sections 5 and 6).

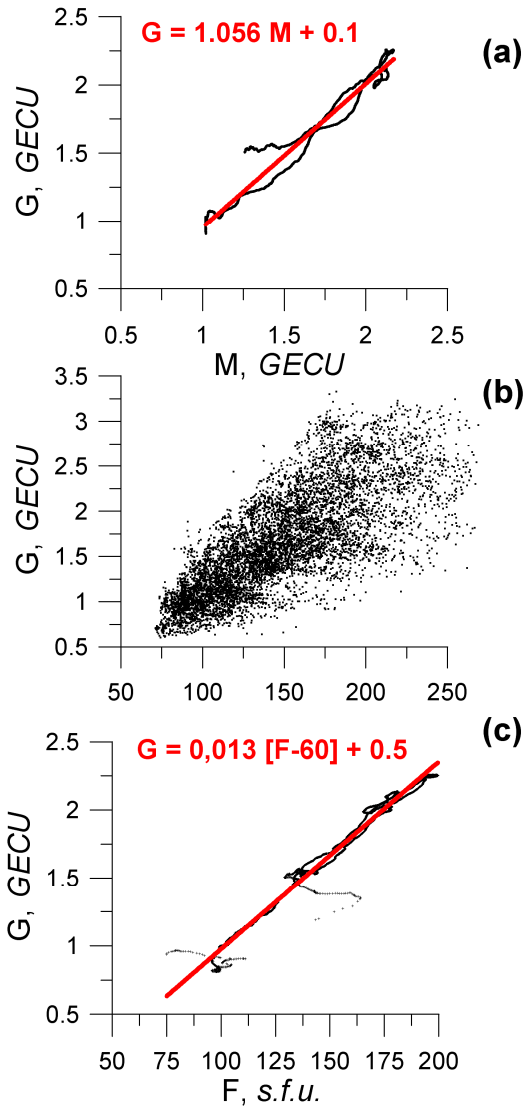

Figure 4: *Regression dependence between GEC G(t) and the 10.7-cm solar radio emission F(t), smoothed with the time windows of 10 days (b) and 365 days (c), respectively. (a) - the same that on (c), but for G(t) and M(t) variations.*

5. Seasonal variations of Global Electron Content

We found that GEC is characterized by strong seasonal (semi-annual) variations with maximum relative amplitude about 10% during the rising and falling parts of the solar activity period and up to 30% during the period of maximum. As one can expect, the semi-annual GEC variations are not correlated with F10.7 variations.

Figure 5c illustrates a comparison between variations of the relative amplitudes dG(t)/G(t) (red curve) and dF(t)/F(t) (green curve) filtered in the time period range from 100 to 300 days. Maximum GEC values were observed at the equinox time. This fact agrees well with the results of studying of a mean TEC dependence over Japan during 2000-2003 (Oyama et al., 2005). This also

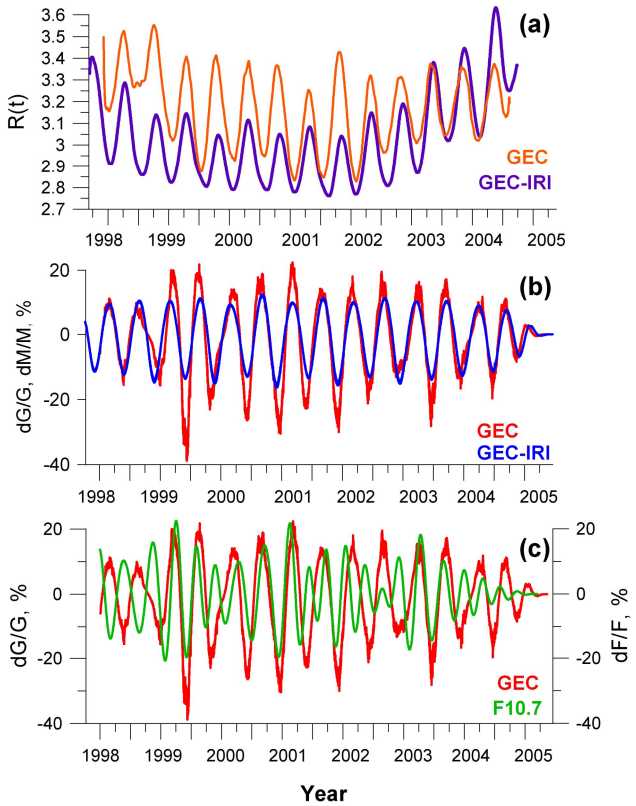

Figure 5: *(a) - the ratio R(t) of the lighted and darken sides of the Earth for G(t) and for M(t); (b) - relative amplitude (%) of G(t) and M(t) variations filtered in the time period range 100-300 days; (c) - the same, but for G(t) (red curve) and F(t).*

is in agreement with the fact that neutral atmosphere density reaches its maximum values in April and October (Krinberg and Taschilin, 1984).

The pronounced seasonal dependence that characterizes the model M(t) series too one can see in Figure 3c (orange curve). Figure 5b illustrates a comparison between variations of the relative amplitudes dG(t)/G(t), % (red curve) and dM(t)/M(t),% (blue curve) filtered in the time period range 100-300 days. We can see similar semi-annual variations of GEC-IRI values with maximum relative amplitude about 10% during the rising and falling parts of the solar activity period and up to 30% during the period of maximum. We found a good agreement between experimental and IRI modeled data for GEC in general, but there are some significant distinctions, which cannot be seen well in 8-year time scale.

Figure 6a presents dependencies of the relative difference between G(t) and M(t) variations (d[G-M]/G, %) smoothed with the 81-day time window, corresponding to 3 rotations of the Sun. This is necessary for smoothing of the 27-day variations of the GEC experimental series caused by solar rotation (see Section 7). The dependencies d[G- M]/G for all years are shown on the same panel .

The mean relative deviations [G(t)-M(t)]/G(t),%, between the experimental G(t) and IRI model series M(t) for all years are shown in Table 2 (lines 2-8). As we can see in Figure 6a and Table 2, the relative difference between G(t) and M(t) variations for some of the years significantly exceed the

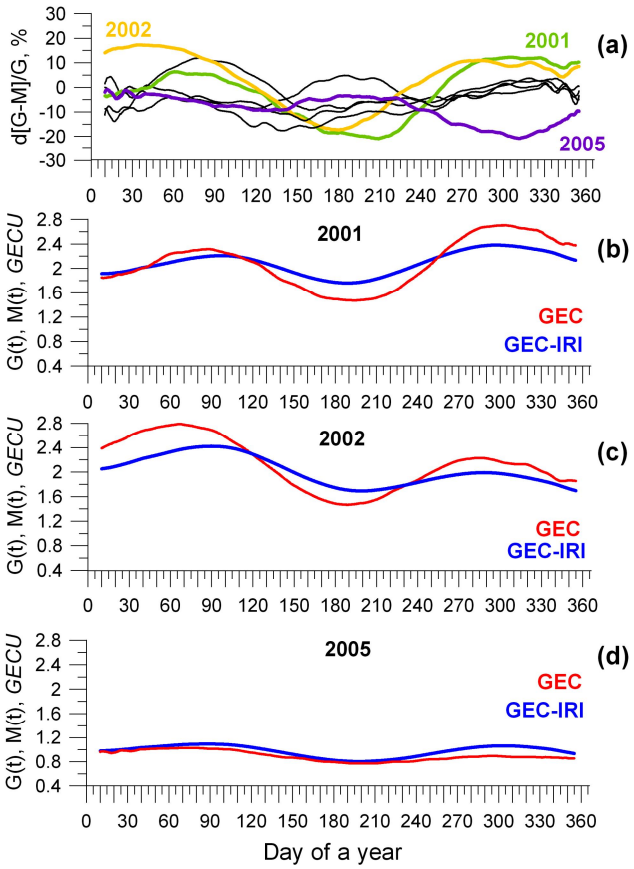

Figure 6: *(a) - 1999-2005 dependencies of the relative difference between G(t) and M(t) variations (d[G-M]/G) smoothed with the 81-day time window; (b-d) - the G(t), and M(t) for the 2001, 2002, 2005.*

difference between series during 1998-2005 smoothed by the one-year time window (Figure 3c and Table 2, line 1).

The dependencies for 2001, 2002 and 2005 years especially stand out. For these years the mean relative difference [G(t)-M(t)]/G(t) reaches 8.6 % (2005) and RMS - up to 10 % (2001, 2002) - see Table 2, lines 7, 3, 4, respectively. Dependencies [G(t)-M(t)]/G(t) for these years are marked by green, yellow and purple colors in Figure 6a respectively, and G(t), M(t) are presented as red and blue curves in panels b, c and d. We found that GEC-IRI seasonal variations are out-of-phase with experimental GEC values. For example, the maximums of the model and experimental curves do not coincide. The lag between model and experimental maximum GEC values can reach several tens of days in the both ways.

6. Global Electron Content of the lighted and darken sides of the Earth

For understanding of the physical mechanisms and comparison with models it is very important to determine GEC for lighted G_d and darken G_n sides of the Earth as well as their ratio $R = G_d/G_n$. For the purpose of G_d and G_n estimation we carry out summation (1) only for those GIM cells that are located inside or outside the solar terminator border determined for a certain altitude H in the atmosphere.

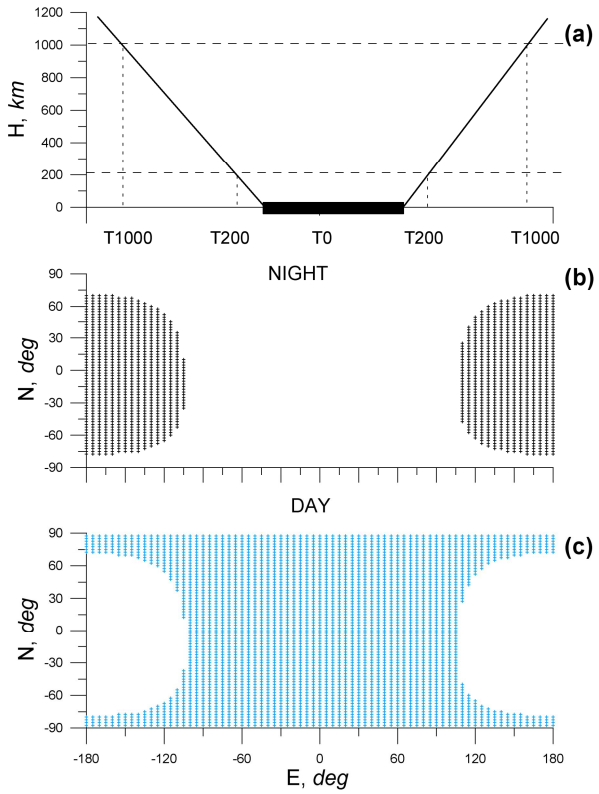

Figure 7: *GEC calculation for the lighted and darken sides of the Earth for different altitude H IRI in the ionosphere (a). Areas for the darken (b) and lighted (c) sides of the Earth for March 31, 2003, and for H=200 km and 12:00 UT, respectively.*

GEC calculation scheme for the lighted and darken sides of the Earth for different altitude H in the ionosphere is shown on Figure 7. Oblique lines mark a shadow boundary at different altitudes in the ionosphere. The area of the lighted zone is bigger as H altitude increases. The lighted zone boundaries T0, T200, T1000 in Figure 7 correspond to altitude values H = 0, 200, 1000 km. Panels (b) and (c) show areas for darken and lighted sides of the Earth for March 31, 2003, for H=200 km and 12 UT, respectively.

Subsequent calculations we have carried out for altitude H = 200 km that is close to the altitude range of the most intensive ionization process of the atmosphere by ultraviolet solar radiation.

Figure 3a presents $G_d(t)$ and $G_n(t)$ values of the lighted and darken sides of the Earth (light blue and black curves) smoothed by 10-day time window. Figure 3c shows the same dependencies M(t) for GEC-IRI values.

Figure 5a shows ratio R(t) of G(t) for the lighted to darken sides of the Earth (orange curve) and M(t) (purple curve) during the 23rd cycle of solar activity (1998-2005). These dependencies are smoothed with 81-day time window. As we can see from Figure 5a, R(t) ratios are effected by deep seasonal variations, however as compared to G(t) (Figure 5b, red curve), the maximum R ratio values are observed during the periods of solstice (in winter and summer). R(t) values changes from 3.1 to 3.7 during the solar activity raise and from 2.8 to 3.5 during the solar activity maximum. A ratio of GEC-IRI of the lighted and darken sides of the Earth is lower (from 2.8 to 3.2) than the one for experimental GEC. Significant distinction of R(t) is at the beginning of the period of analysis (1998-2001).

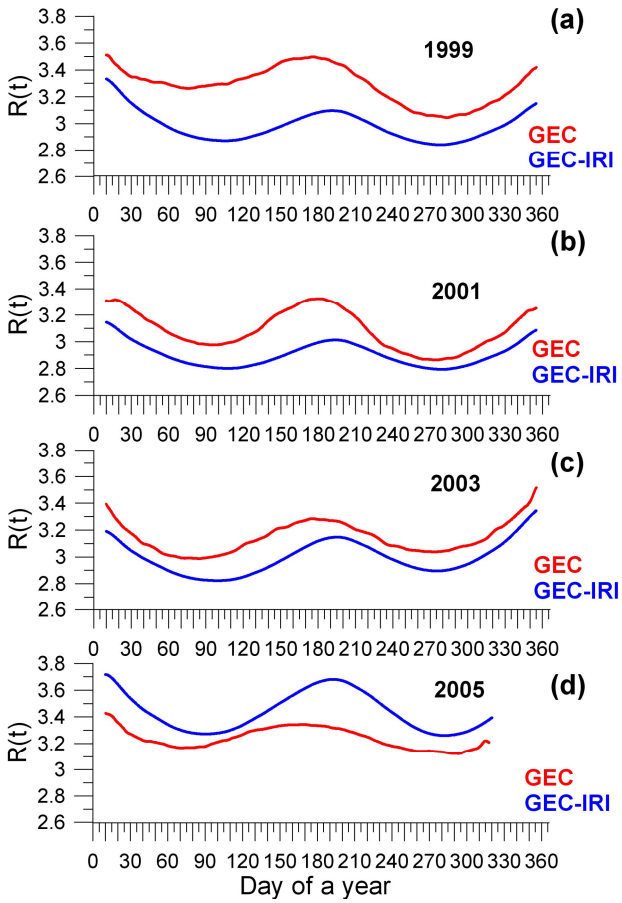

Figure 8: *A ratio R(t) of the lighted and darken sides of the Earth of G(t) (red curves) and of M(t) (blue curves) for the 1999, 2001, 2003, 2005.*

Figure 8 illustrates difference between experimental and model values R(t) in detail within the time scale for 1 year (a - 1999; b - 2001; c - 2003, d - 2005). It is obvious from the figures that IRI produces underestimated values of the ratio R(t) for G(t), i.e. the value of the darken side ionization is significantly overestimated. Besides as like for seasonal variations of G(t) (Figure 6), the phase shift of the seasonal variations of the ratio R(t) is observed.

7. 27-day variations of Global Electron Content

One of the main factors of solar radiation influence on the ionosphere state is quasi 27-days variations caused by solar rotation. A lot of works have been devoted to research of this factor (Akasofu and Chapmen, 1972; Ivanov-Kholodny and Nikolsky, 1969; Vitinsky et al., 1986; Jakowski et al., 1991, 1998, 2002). However, quasi 27-day modulation of local ionosphere parameters can be masked by many other factors. The latter makes impossible to derive reliable numerical characteristics of the 27-day variations of the solar ultraviolet radiation. Global electron content reflects more clearly this feature of solar ultraviolet radiation.

Figure 9 shows time dependencies of relative amplitude dG/G,% of 27-day variations for G(t) and of F10.7 for F(t). GEC variations were calculated for each day within the interval from 17.00 to 21.00 UT. Figure 9 presents G(t) variations for the entire globe (c, orange curve), G(t) of the lighted

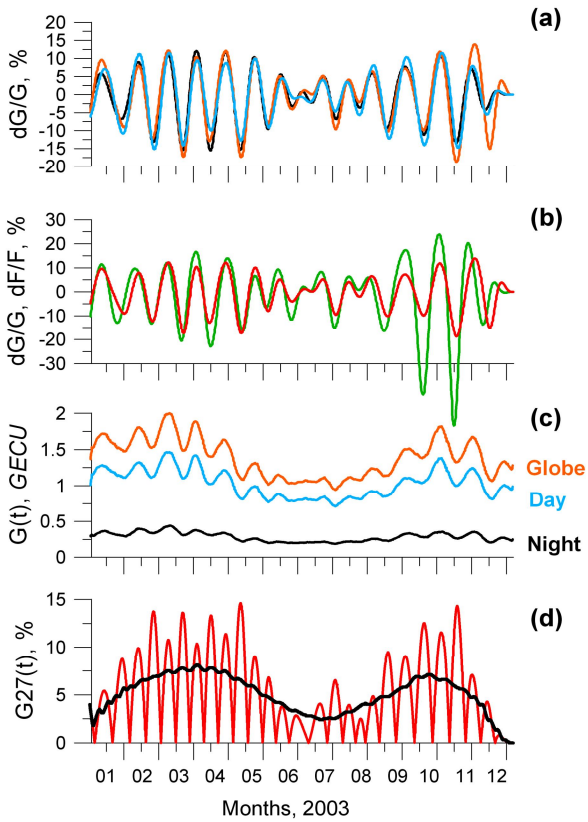

Figure 9: *Relative amplitude of 27-day variations of G(t) and F(t), filtered in the time period range 20-40 days: (a) - dG/G(t); (b) - G(t) and F(t); (c) - G(t) variations for the entire globe (orange curve), G(t) of the lighted and darken sides of the Earth. Panel (d) illustrates the calculation procedure of the envelope G27(t) of 27-day GEC variations.*

and darken sides of the Earth (c, light blue and black curves), smoothed with the 10-day time window (for the year 2003). The series were filtered within the period range from 20 to 40 days and normalized on background values of the G(t) and F(t). Because of limited paper size, we illustrate the dependence only for the 2003. Relative amplitude of 27-day variations of G(t) and F(t) are shown on panel (b): G(t) for the globe, red curve; F(t), green curve, and on panel (a) - dG/G(t) for the entire globe (orange curve) and of the lighted (light blue curve) and darken (black curve) sides.

Correlation analysis for all data from 1998 to 2005 displays high similarity between 27-day variations of the G(t) and F(t) (maximum correlation coefficient is more than 0.8). Besides, we found that 27-day GEC variations lag for 1.5-2.5 days after the corresponding F10.7 variations (Figure 9b). At the same time 27-day GEC variations for the globe and on the lighted and darken sides of the Earth are in phase with each other (Figure 9a).

It is known that response of the ionosphere to ultraviolet radiation flux changes is determined by the lag time and the recombination time constants, which is equal about 1 hour (Ivanov-Kholodny and Nikolsky, 1969; Bryunelli and Namgaladze, 1988). Founded lag of the 27-day GEC variations relative to corresponding changes of the F10.7 flux can be caused by significantly greater time constants that characterize thermosphere as GEC variations are caused not only by changes of the solar ionizing radiation but the processes in the thermosphere. As solar radiation flux increases, ionizing the ionosphere and heating the thermosphere, the temperature and total density of the atmosphere increase, and the speed and direction of the neutral wind are changed (Bryunelli and

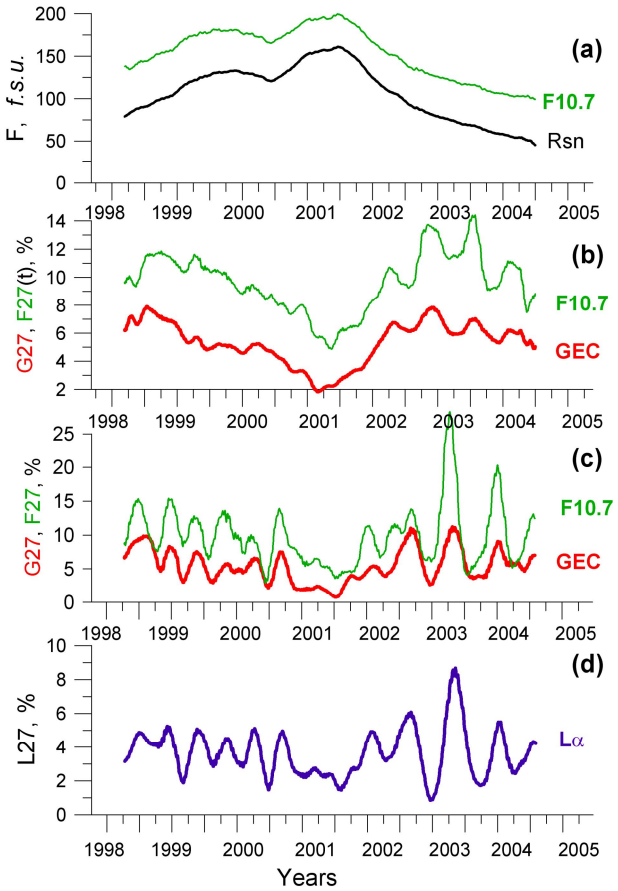

Figure 10: *The envelope of 27-day variations G27(t) of GEC and F27(t) of the 10.7-cm solar radio emission – (b, c); (d) - emission of Lyman-alpha irradiance; (a) - dependencies of the 10.7-cm solar radio emission F(t) and daily value sunspot number Rsn.*

Namgaladze, 1988). It is also necessary to take into account that time scales of the electron content variations in the Earth's plasmasphere are changed within the range from 2 to 5 days (Krinberg and Taschilin, 1984). Detailed analysis of the factors responsible for the founded lag of 27-day GEC variations relative to corresponding changes of the F10.7 flux is a very difficult point, and it is out of the scope of this paper.

Estimation of 27-day variations amplitude envelope during the solar activity period is of importance. Figure 9d illustrates the procedure of calculation of the envelope G27(t) for relative amplitude dG/G(t) of 27-day GEC variations shown in Figure 9b by red curve. First of all, we square the dependence dG/G(t) (fig. 9d, red curve). Then, we smooth the envelope of $[dG(t)/G(t)]^2$ by 81-day time window (black curve).

Figure 10 presents the envelope of 27-day variations of GEC (G27(t), red curves) and of 10.7-cm solar radiation flux (F27(t), green curves) during the 23rd cycle of solar activity (1998-2005), smoothed by 365-day time window (b) and 81-day window (c). Panel (d) shows the same as panel (c), but for solar Lyman-alpha irradiance at 121.67 nm (http://www.spacewx.com).

For comparison, panel (a) shows smoothed dependencies of 10.7-cm solar radiation flux F(t) (green curve), the daily value of the derived sunspot number Rsn (black curve) during 1998-2005 (http://www.spacewx.com). It is seen that maximal deviation of the relative amplitude G27(t)

Table 2: *Results of comparison between GEC-IRI and experimental GEC values.*

N	Year	Time window, days	(G-M)/G, %	RMS, %
1	1998-2005	365	-1,5	5,0
2	1999	81	-1,4	4,3
3	2000	81	-1,3	7,0
4	2001	81	-1,6	10,7
5	2002	81	3,6	10,0
6	2003	81	-7,1	5,7
7	2004	81	-6,1	3,4
8	2005	81	-8,6	5,6
9	1999	10	-1,98	10,5
10	2000	10	-1,98	11,0
11	2001	10	-2,81	15,1
12	2002	10	2,88	13,7
13	2003	10	-7,8	11,0
14	2004	10	-6,5	8,6
15	2005	10	-9,3	9,2

decreases from 8% at the rising and falling solar activity to 2% at the period of its maximum. Such dependence is caused by active formations on the Sun surface, which number increases as solar activity increase (Mordvinov and Plyusnina, 2001; Mordvinov and Willson, 2003). At the same time magnitude of 27-day ultraviolet radiation flux modulation decreases.

On the contrary, during solar activity falling period “frozen-in” intensive active formations arise at the Sun, which can exist during some rotations of the Sun (Vitinsky et al., 1986; Mordvinov and Plyusnina, 2001; Mordvinov and Willson, 2003). This is especially obvious in the case of smoothed series of the relative amplitude of 27-day variations by 81-day time window. Thus, during the 23rd cycle end (2003, 2004) the F10.7 variations amplitude can reaches 25% (Figure 10c).

The IRI-2001 model does not take into account the 27-day variations of F10.7. Nevertheless it is interesting to estimate the mean relative deviation [G(t)–M(t)]/G(t), between experimental G(t) smoothed by 10-day time window and IRI model series M(t) for all the years under consideration. These data are presented in Table 2 (lines 9-15).

As shown in Table 2 the relative difference between G(t) and M(t) variations for some years essentially exceeds the difference between series during 1998-2005 smoothed by one-year time window (line 1). The same we can say about seasonal variations G(t) and M(t) (lines 2-8). So the mean relative difference [G(t)-M(t)]/G(t) increases to the end of 23rd cycle and reaches 9.3% (2005). However RMS [G(t)-M(t)]/G(t) is maximum for the period of solar activity maximum: 15.1% (2001) and 13.7% (2002).

8. Conclusion

1. We present the first results for investigation the dynamics of global electron content that is equal to the total number of electrons in the near space bounded by the GPS orbital altitude. We propose the method of GEC estimation based on the Global Ionospheric Maps technique.

2. The systematic deviations were found between GEC values calculated on the base of the different laboratories IONEX data presented in the Internet (JPLG, CODG, ESAG, UPCG).

3. During the period 1998-2005 the average level of GEC varied from 0.5 to 3.5 GECU. 27-day variations of GEC are very similar to the ones of the index F10.7, but GEC undergoes a lagging of about of 30-60 hours. GEC has seasonal variations with maximum values in equinoctial months. Deep seasonal variations are also typical for a ratio of GEC for the lighted and darken sides of the Earth. Maximal values of this ratio were observed during the periods of summer and winter solstices.

4. We developed the method and software for GEC estimation using IRI-2001 (GEC-IRI) and compared its results with experimental GEC values during the period from 1998 to 2005. Good agreement between observational and model data for GEC was found in general, but there are some distinctions.

5. Significant overestimation of GEC-IRI values is perceptible for upper integration heights higher than 2000 km (up to 5-6 times for GPS satellites altitude, 20000 km).

6. Relative difference and RMS between GEC-IRI and experimental GEC series increase as smoothing time window decreases. Mainly this reflects the fact that IRI is a median ionosphere model and do not take into account day-to-day variations of the ionosphere parameters (e.g. 27-day variations).

Thus, the data obtained in this study should be of considerable interest for calibration and correction of IRI by using GEC data. The results are also important for studying of the ionization balance caused by solar ultraviolet radiation and by charged particle precipitation in the auroral zones. Combined with the data from the worldwide network of ionosondes, our results can be used in estimating the contribution of the plasmasphere to total electron content.

10. Contact Information

E.L. Afraimovich, E.I. Astafyeva, A.V. Oinats or Yu.V. Yasukevich

Institute of Solar-Terrestrial Physics SD RAS
Box 4026
126, Lermontov Str.
Irkutsk, 664033, Russian Federation
E-mail: afra@iszf.irk.ru
Phone: +7 (3952) 56 45 54
FAX: +7 (3952) 51 16 75
WWW: http://rp.iszf.irk.ru/homepage/afra/

I.V. Zhivetiev

Institute of Cosmophysical Research and Radiowave Propagation, FED RAS
Petropavlovsk-Kamchatskii, Russian Federation

Acknowledgements

We acknowledge academician G.A. Zherebtsov, Drs. V.V. Pipin, V.G. Eselevich, A.V. Mordvinov, L.A. Plyusnina for their support and interest in our work and E.A. Kosogorov for his help in programming. We are grateful to N. Jakowski, D. Bilitza, S.M. Radicella for their interest in our work and good suggestions.

We acknowledge for the IONEX data presented in Internet: Center for Orbit Determination in Europe, University of Berne, Switzerland (CODG), Jet Propulsion Laboratory of California Institute of Technology (JPLG), Grup Universitat Politecnica de Catalunya (UPCG), European Space Agency Group (ESAG).

The work was done under support of the Russian Foundation for Basic Research (grant No. 05-05-64634).

References

Akasofu, S.I., Chapmen, S., 1972. Solar-Terrestrial Physics. Pergamon, Oxford.

Afraimovich, E.L., Chernukhov, V.V., Demyanov, V.V., 2000. Updating the ionospheric delay model for single-frequency equipment of users of the GPS. Radio Sci. 35(1), 257-262.

Afraimovich, E.L., Astafyeva, E.I., Zhivetiev, I.V. Solar activity and global electron content. 2006. Doklady Earth Sciences (accepted).

Beynon, W.J.G., Brown, G.M., 1959. Region E and solar activity. J. Atm. Phys. 15, 168-174.

Bhuyan, P.K., Rashmi Rekha Borah, 2005. TEC derived from GPS network in India and comparison with models. Proceedings of the GA URSI'2005, Delhi, India (http://www.ursi.org/Proceedings/ProcGA05/pdf/GF1a.6(0754).pdf).

Bilitza, D., 1990. International Reference Ionosphere 1990. NSSDC 90-22, Greenbelt, Maryland.

Bilitza, D., 2001. International reference ionosphere. Rad. Sci. 36(2), 261-275.

Bilitza, D., 2004. A correction for the IRI topside electron density model based on Alouette/ISIS topside sounder data. Adv. Space Res. 33(6), 838-843.

Bryunelli, B.E., Namgaladze, A.A., 1988. Physics of the Ionosphere. Nauka, Moscow.

Coisson, P., Radicella, S.M., Nava, B., 2002. Comparisons of experimental topside electron concentration profiles with IRI and NeQuick models. Annals of geophysics 45(1), 111-116.

Coisson, P., Radicella, S.M., 2004. The IRI topside parameters. Adv. Radio Sci. 2, 249-–251.

Coisson, P., Radicella, S.M., 2005. Ionospheric topside models compared with experimental electron density profiles. Annals of geophysics 48(3), 497-503.

Coisson, P., Radicella, S.M., Leitinger, R., Nava, B., 2005. New option for IRI topside electron density profile using NeQuick model. IRI NewsLetter 12 (1,2,3), 5-7.

Daniell, Jr., R.E., L.D. Brown, D.N. Anderson, M.W. Fox, P.H. Doherty, D.T. Decker, J.J. Sojka, and R.W. Schunk, 1995. Parameterized ionospheric model: A global ionospheric parameterization based on first principles models, Radio Sci., 30, 1499-1510.

Gallagher, D.L., P.D. Craven, and R.H. Comfort, 1988. An empirical model of the earth's plasmasphere, Adv. Space Res., 8, 15-24.

Giovanni, G., Radicella, S.M., 1990. An analytical model of the electron density profile in the ionosphere. Adv. Space Res. 10(11), 27-30.

Hofmann-Wellenhof, B., H. Lichtenegger, J. Collins, 1992. Global Positioning System: Theory and Practice. Springer-Verlag Wien, New York, 327 p.

Huang, X., Reinisch, B.W., Bilitza, D., and Benson, R. F., 2002. Electron density profiles of the topside ionosphere. Annals of Geophysics 45(1), 125–130.

Ivanov-Kholodny, G.S., Nikolsky, G.M., 1969. The sun and ionosphere. Nauka, Moskow.

ITU (2004): Ionospheric propagation data and prediction methods required for the design of satellite services and systems. Recommendation ITU-R P.531-7.

Jakowski, N., Fichtelmann, B., Jungstand, A., 1991. Solar activity control of Ionospheric and thermospheric processes. J. Atmosp. Terr. Phys. 53, 1125-1130.

Jakowski, N., Sardon, E., Schluter, S., 1998. GPS-based TEC observations in comparison with IRI95 and the european TEC model NTCM2. Adv. Space Res. 22, 803-806.

Jakowski, N., Heise, S., Wehrenpfennig, A., Schluter, S., Reimer, R. 2002. GPS/GLONASS-based TEC measurements as a contributor for space weather. J. Atmosp. Sol.-Terr. Phys. 64(5-6), 729-735.

Klobuchar, J.A., 1986. Ionospheric time-delay algorithm for single-frequency GPS users. IEEE Transactions on Aerospace and Electronics System 23(3), 325-331.

Krinberg, I.A., Taschilin, A.V., 1984. Ionosphere and Plasmosphere. Nauka, Moscow. Leitinger, R., Zhang, M., Radicella, S.M., 2005. An improved bottomside for the ionospheric electron density model NeQuick, Annals of geophysics 48(3), 525-534.

Mannucci, A.J., Wilson, B.D., Yuan, D.N., Ho, C.M., Lindqwister, U.J., Runge, T.F., 1998. A global mapping technique for GPS-derived ionospheric TEC measurements. Radio Sci. 33(3), 565-582.

Mordvinov, A.V., Plyusnina, L.A., 2001. Coherent structures in the dynamics of the large-scale solar magnetic field. Astronomy reports 45, 652-658.

Mordvinov, A.V., Willson, R.C., 2003. Effect of large-scale magnetic fields on total solar irradiance. Sol. Phys. 215, 5-16.

Nusinov, A.A., 2004. The Ionosphere as a Natural Detector for Studying Long-Period Variations in the Fluxes of Solar Geoeffective Radiation. Geomagn. Aeron. 44(6), 718–725.

Oyama K.-I., Noguchi K., Izawa M., Saito A., Otsuka Y., and Tohyama F., 2005. Local time, annual, latitude, and seasonal variations of total electron content over Japan. Institute of space and astronautical science. ISAS Research Note 796.

Radicella, S.M., Leitinger, R., 2001. The evolution of the DGR approach to model electron density profiles. Adv. Space Res. 27(1), 35-40.

Schaer, S., Beutler, G., Rothacher, M., 1998. Mapping and predicting the ionosphere. Proceedings of the IGS AC Workshop, Darmstadt, Germany.

Vitinsky, Yu.I., Kopecky, M., Kuklin, G. V., 1986. Statistics of sunspot activity. Moscow: Nauka, p. 296.